Available online at www.sciencedirect.com
SCIENCE DIRECT
Journal of Catalysis 239 (2006) 441–450
JOURNAL OF CATALYSIS
www.elsevier.com/locate/jcat

Methane dehydroaromatization under nonoxidative conditions over Mo/HZSM-5 catalysts: Identification and preparation of the Mo active species

Hongmei Liu [a,b], Xinhe Bao [a], Yide Xu [a,*]

[a] *State Key Laboratory of Catalysis, Dalian Institute of Chemical Physics, Chinese Academy of Sciences, 457 Zhongshan road, P.O. Box 110, Dalian 116023, China*

[b] *Key Laboratory of Organic Optoelectronics & Molecular Engineering, Department of Chemistry, Tsinghua University, Beijing 100084, China*

Received 11 November 2005; revised 17 February 2006; accepted 21 February 2006

Available online 24 March 2006

Abstract

Complete reduction of Mo species interacting strongly with a HZSM-5 zeolite support in methane is difficult, and the reduction product, MoC_xO_y, is a key active species in methane dehydroaromatization (MDA) under nonoxidative conditions. Pretreatment in H_2 at 623 K could lead to topotactic transformation of the Mo species from hexagonally close packing (hcp) to face-centered cubic (fcc) structures; the fcc MoC_xO_y species are more active and more stable than the hcp MoC_xO_y in MDA. After initial H_2 pretreatment at 623 K, followed by a CH_4-treatment, the Mo species on a MoO_3/HZSM-5 catalyst prepared by mechanical mixing was reduced and carburized to form fcc α-MoC_{1-x} species on the extra surface of the zeolite. Methane molecules activated by the α-MoC_{1-x} were converted mainly into carbon deposits instead of benzene. Both the most active Mo species and the neighboring Brönsted acid sites are essential in obtaining a perfect catalyst in the reaction of MDA.

Keywords: Methane; Aromatization; ZSM-5; Molybdenum; Reduction

1. Introduction

Methane dehydroaromatization (MDA) in the absence of gas-phase oxygen has received considerable recent attention as a promising route for direct conversion of methane into highly value-added chemicals [1–3]. Up to now, most research work has focused on Mo/HZSM-5 catalysts, prepared by either the impregnation or the solid-state reaction method. It is generally accepted that both the activation of the methane C–H bond and the formation of the initial C–C bond occur on the reduced Mo carbide species, which is formed from the reduction of MoO_x species by CH_4 in the early stage of the reaction, whereas the oligomerization, cyclization, and aromatization of the C_2 hydrocarbon species are catalyzed by the Brönsted acid sites of the HZSM-5 zeolite [4–18].

Several kinds of Mo species on/in the Mo/HZSM-5 catalysts existing in different states and various coordination environments were identified by FTIR, ISS, NH_3-TPD [4,9,19], NH_4OH extraction, and ^{27}Al and ^{29}Si MAS NMR techniques [8,9]. Usually, the Mo oxide species are highly dispersed on the HZSM-5 surface and interact with the Brönsted acid sites of the HZSM-5 if the Mo loading is <8 wt% and the calcination temperature is below 823 K. With increasing Mo loading, MoO_3 crystallites can be detected by XRD and FTIR [4]. However, the tendency of framework Al extraction by Mo oxide species becomes more significant with increased Mo loading and elevated calcination temperature. What kind of Mo oxide species acts as the precursor of the active Mo carbide species in MDA remains under debate. Solymosi and coworkers [5–7] and Lunsford and coworkers [20,21] in their early stage of research for this topic, have suggested that the Mo_2C species, highly dispersed on the external surface of the HZSM-5 zeolite, are the active sites and are responsible for the initial methane activation. Recently, Iglesia and coworkers found that after cal-

* Corresponding author. Fax: +86 411 84694447.
E-mail address: xuyd@dicp.ac.cn (Y. Xu).

0021-9517/$ – see front matter
doi:10.1016/j.jcat.2006.02.018

cination at 773 K under specified conditions, all of the Mo species replaced the Brönsted acid sites with a stoichiometry of 1:1 and existed in the channels of the HZSM-5 zeolite [22–25]. They also found that the Mo species in the channels were more effective in the activation of methane and less sensitive in the formation of carbonaceous deposits [26]. Our previous studies have demonstrated differing reducibilities of the Mo species located at various positions of the HZSM-5 zeolite; that is, the MoO_x species that were not associated with the Brönsted acid sites could be easily and fully reduced into the Mo carbide species by methane, whereas the Mo species associated with the Brönsted acid sites could be only partially reduced by CH_4 to form MoO_xC_y species [27].

In this work, we studied the effect of hydrogen prereduction of Mo/HZSM-5 catalysts prepared by different methods (i.e., impregnation and mechanical mixing) at low temperature (623 K) on the structure and the catalytic performance of MDA. EPR was used to monitor and characterize the alteration in chemical environment and coordination situation of the Mo species during prereduction and at the early reaction stage.

2. Experimental

2.1. Catalyst preparation

MoO_3/HZSM-5 samples with a Mo loading of 6 wt% were prepared by traditional impregnation or mechanical mixing. With the traditional impregnation method, the HZSM-5 zeolite (supplied by Nankai University, $SiO_2/Al_2O_3 = 50$) was impregnated with an aqueous solutions containing the desirable amount of ammonia heptamolybdate ($(NH_4)_6[Mo_7O_{24}]\cdot 4H_2O$), and then dried at room temperature for 12 h. Finally, it was dried at 393 K for 2 h and calcined in air at 773 K for 6 h. With the mechanical mixing method, HZSM-5 zeolite was thoroughly mixed with a given amount of MoO_3 powder (analytical grade, obtained from Beijing Shuanghuan Weiye Reagent Co. Ltd; $S_{BET} = 7\ m^2/g$), and then was ground in an agitating mortar for 30 min. The catalyst prepared by impregnation was denoted as im-MoO_3/HZSM-5; that prepared by mechanical mixing, as mm-MoO_3/HZSM-5. When used as samples for catalyst evaluation and characterization, the catalyst was crushed and sieved to 250–425 μm granules (20–60 mesh).

2.2. Catalyst activation pretreatments

Before the reaction, MoO_3/HZSM-5 was prereduced in situ by H_2. A 0.2-g sample was charged into a fixed-bed quartz tubular reactor (6.2 mm i.d.), and a hydrogen flow of 2400 ml/(g_{cat} h) was introduced into the reactor. After the H_2 prereduction, a 10% N_2/CH_4 stream with a space velocity of 1500 ml/(g_{cat} h) was introduced into the reactor, and the temperature was raised to 973 K at a rate of 5 K/min. All gases used in this work were of UHP grade and were used without further purification. The catalyst prereduced with H_2 at 623 K was denoted as MoO_x/HZSM-5. The real catalyst, prereduced at 623 K and then heated in a 10% N_2/CH_4 stream to the reaction temperature of 973 K, was denoted as Mo/HZSM-5(H), whereas the catalysts that had no H_2 prereduction and was heated directly in a 10% N_2/CH_4 stream was denoted as Mo/HZSM-5(M).

2.3. Catalyst evaluation

After the in situ activation pretreatment, the catalyst was evaluated in a gas mixture of 10% N_2/CH_4 (1500 ml/(g_{cat} h)) at 973 K and under atmospheric pressure. The feed was a gas mixture of 10% N_2/CH_4 (1500 ml/(g_{cat} h)), and the N_2 in the CH_4 was used as an internal standard, as reported by Lunsford et al. [21], for measuring the CH_4 conversion as well as the selectivity of all products and carbonaceous deposits. On-line analysis of the effluent was performed with a Hewlett-Packard 6890 gas chromatograph. The hydrocarbon products, including ethane, ethylene, and condensable C_6–C_{10} aromatics (e.g., benzene, toluene, xylene, and naphthalene), were separated by using a methyl-silicone HP-1 capillary column (0.32 mm × 50 m) and analyzed by a flame ionization detector (FID). On-line separation and analysis of H_2, N_2, CO, CH_4, CO_2, C_2H_4, and C_2H_6, were done with a HayeSep-D column (3 mm × 2 m) and a thermal conductive detector (TCD) on the same gas chromatograph. Methane conversion, hydrocarbon product selectivity, and coke formation were evaluated according to carbon mass balance. All reaction rates were calculated basing on carbon balance and expressed as mmol/(g_{cat} s).

2.4. Catalyst characterization

Temperature-programmed reduction (TPR) was carried out in a setup TP-5000-II setup equipped with a TCD detector. The sample charge was 0.05 g and it was first pretreated under a N_2 stream at 873 K for 30 min or in a hydrogen flow at 623 K for 6 h, and then cooled to room temperature. An H_2/N_2 stream (5% H_2, 20 ml/min, UHP) was passed over the sample while it was being heated from room temperature to 1173 K at a rate of 10 K/min.

X-Ray photoelectron spectroscopy (XPS) measurements were performed using a Leybold LHS 12 MCD system with an Al-K_α radiation source, operated at 300 W. After the sample was pretreated in a hydrogen flow of 2400 ml/(g_{cat} h) at 623 K for 6 h, if necessary, the Mo 3d and C 1s XPS spectra were collected using pass energy of 100 eV. The electron binding energies (BEs) were referenced to the C 1s peak at 284.60 ± 0.05 eV.

Electron paramagnetic resonance (EPR) experiments were performed on a JEOL ES-EO3X X-band spectrometer at room temperature. A microwave frequency γ of 9.42 GHz and a power of 1 mW were used. The relative spin concentration and the g factor were calculated using the signal of manganese as an internal standard. A specially designed EPR flow reactor cell that could be placed in the resonance cavity was used. The reactor cell for EPR measurements was made of quartz (4 mm i.d.,) and was normally charged with 0.2 g of catalyst sample. With this reactor cell, real fixed-bed catalytic reaction conditions could be simulated. The MoO_3/HZSM-5 catalyst was pre-

Table 1
Numerical results of TPR experiments on MoO_3/HZSM-5 and MoO_x/HZSM-5 catalysts prepared by different methods and pre-activated through different procedures

Sample		Peak 1	Peak 2	Peak 3	Peak 4
im-MoO_3/ HZSM-5	Peak temperature (K)	784	877	945	1023
	The amount of hydrogen consumption (μmol/g_{cat})	***364***	***300***	***176***	***375***
im-MoO_x/ HZSM-5	Peak temperature (K)	787	889	976	1054
	The amount of hydrogen consumption (μmol/g_{cat})	***311***	***287***	***170***	***371***
mm-MoO_3/ HZSM-5	Peak temperature (K)		824		1007
	The amount of hydrogen consumption (μmol/g_{cat})		***599***		***1185***
mm-MoO_x/ HZSM-5	Peak temperature (K)		817		1000
	The amount of hydrogen consumption (μmol/g_{cat})		***391***		***1127***

reduced with H_2 (2400 ml/(g_{cat} h)) at 623 K for 6 h if necessary. Then a methane stream (1500 ml/(g_{cat} h)) was introduced into the reactor cell, and the temperature was increased to 973 K. After the reaction or prereduction, the reactor was transferred into the resonance cavity of the EPR spectrometer under a protecting gas. The EPR signals were recorded during the processes of H_2 pretreatment and methane treatment, respectively. The EPR spectra were digitized and doubly integrated by the PEAKFIT workstation to calculate the relative spin concentration.

Temperature-programmed surface reaction of methane (CH_4-TPSR) was carried out in a U-shaped quartz tubular microflow reactor. Before measurement, the catalyst (0.2 g) was heated from room temperature to 873 K in a He stream at a rate of 10 K/min and held at 873 K for 30 min to remove the water absorbed on the sample. After cooling to room temperature, the pretreatment and the MDA reaction were performed under the same conditions as in a real fixed-bed reactor. Meanwhile, the effluent were analyzed on-line by a Balzers QMS-200 multichannel quadruple mass spectrometer for m/e of 2(H_2), 16(CH_4), 18(H_2O), 27(C_2H_4), 28(CO), 44(CO_2), and 78(C_6H_6).

Temperature-programmed oxidation (TPO) measurements were carried out after the CH_4-TPSR experiment, using the same apparatus. After cooling to room temperature, the used catalyst was heated from room temperature to 1073 K in a stream of 10% O_2/He (30 ml/min) at a rate of 20 K/min. During the temperature ramp, MS intensities for carbon oxides (CO and CO_2) were measured as a function of temperature. The TPO profiles were calculated as described previously [28,29].

3. Results

3.1. TPR and XPS results

The TPR results are listed in Table 1. The im-MoO_3/HZSM-5 sample without H_2 pretreatment exhibited four peaks, at 784, 877, 945, and 1023 K. As has been reported, the peak at 784 K is usually attributed to the reduction of MoO_3 to MoO_2, which was well dispersed on the external surface of HZSM-5 zeolite, whereas the hydrogen consumption signal at 945 K was generally assigned to the further reduction of the well-dispersed MoO_2 species [30,31]. It should be noted that the amount of hydrogen consumption corresponding to the TPR peak at 945 K was about 1/2 of that corresponding to the peak at 784 K, indicating that most Mo^{4+} species could not be thoroughly reduced to Mo^0. Recently, Xu et al. [27] suggested that two kinds of Mo species are located on a MoO_3/HZSM-5 catalyst prepared by impregnation, one kind located on the external surface of the zeolite that can be readily reduced and the other kind associated with framework Al that is difficult to reduce. It is reasonable to ascribe the TPR peak at 877 K to the initial reduction of the second kind of Mo^{6+} species to Mo^{4+}, whereas the signal at 1023 K can be assigned to the further reduction of the Mo^{4+} species associated with Brönsted acid sites.

The im-MoO_x/HZSM-5 sample, which was pretreated in hydrogen at 623 K for 6 h in advance, also exhibited four hydrogen consumption peaks in the TPR profile. The hydrogen consumption amounts corresponding to the two low-temperature signals of the im-MoO_x/HZSM-5 catalyst are slightly smaller than those of the im-MoO_3/HZSM-5 catalyst without H_2 pretreatment. This indicates that the Mo species located on the external surface and those associated with the Brönsted acid sites can be partially reduced during the in situ pretreatment in hydrogen at 623 K for 6 h.

Two signals, at 824 and 1007 K, are shown in the TPR profile of a fresh mm-MoO_3/HZSM-5 catalyst, with the amount of hydrogen consumption at the higher temperature double that at the lower temperature. The two peaks correspond to the reduction of aggregative crystalline MoO_3 to MoO_2 and a further complete reduction to metal Mo species, respectively [32,33]. Comparatively, no new hydrogen consumption signals were present in the TPR profile of the mm-MoO_x/HZSM-5 sample, indicating that the Mo species were still located on the external surface of the HZSM-5 zeolite and had not migrated into the channels even after the pretreatment at 623 K. However, the intensity of the signal at the lower temperature decreased dramatically, suggesting that some of the Mo species were reduced during H_2 pretreatment.

The Mo 3d XPS spectra of the im- and mm-MoO_3/HZSM-5 catalysts without H_2 pretreatment displayed only one state of molybdenum, that is, the Mo^{6+} species with a typical doublet at 235.8 and 232.6 eV (spectra not shown here), consistent with the literature data for MoO_3 species supported on HZSM-5 zeolite [9,34–36]. After the samples were treated with hydrogen at 623 K for 6 h, the XPS spectra showed a more complicated structure. Curve fitting revealed the disappearance of a part of the Mo^{6+} oxidation state and the appearance of a Mo^{5+} spin-orbit component. The BE values for the Mo 3d of the Mo^{5+} species were recorded at 234.7 and 231.5 eV [35], demonstrating that part of the Mo species could be reduced in hydrogen to form Mo^{5+} species on either im-MoO_3/HZSM-5 or mm-MoO_3/HZSM-5.

3.2. EPR characterization of the Mo species on im-MoO_3/HZSM-5 samples

No signals could be observed in the EPR spectrum of a fresh MoO_3/HZSM-5 catalyst prepared by impregnation, in-

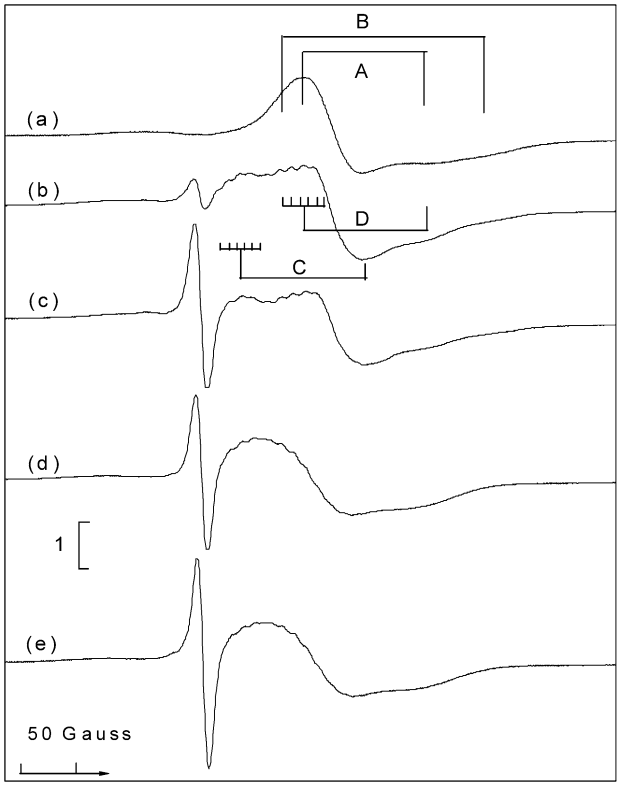

Fig. 1. EPR spectra of the im-MoO_3/HZSM-5 sample after prereduced with H_2 at 623 K for 6 h (a), and the im-Mo/HZSM-5(H) catalyst after running the MDA for 0.5 h (b), 1 h (c), 2 h (d), and 4 h (e) at 973 K.

dicating the diamagnetism of the Mo^{6+} species. However, as shown in Fig. 1a, the EPR spectrum of the im-MoO_x/HZSM-5 sample, obtained by treating im-MoO_3/HZSM-5 at 623 K for 6 h, shows two smooth and axially symmetric EPR signals that overlap. For simplification, the signals located at $g_\perp = 1.950$, $g_\parallel = 1.894$ and $g_\perp = 1.959$, $g_\parallel = 1.866$ are denoted as A and B, respectively. The shapes and g values of signals A and B are very similar to the EPR signals of the Mo^{5+} species formed on various supported molybdenum-based catalysts as well as on these species after different reduction treatments, as reported previously [37–41]. Che et al. [40,41] have suggested that both of the two Mo^{5+} species, corresponding to the signals A and B, have a short Mo=O bond and are surrounded only by oxygen ligands. The signal A is attributed to the Mo^{5+}_{6c} species with distorted octahedral coordination symmetry, whereas the signal B is assigned to the Mo^{5+}_{5c} species in the form of square pyramidal coordination [40,41]. After the sample was prereduced with H_2 at 623 K for 6 h, signals of both the Mo^{5+}_{6c} and Mo^{5+}_{5c} species appeared, indicating that the Mo^{6+} species can be reduced readily to Mo^{5+}, in the form of either compressed octahedral coordination or square pyramidal coordination. Xu et al. [27] have reported that when a 2 wt% MoO_3/HZSM-5 catalyst was reduced in a methane stream at 573 K for 1 h, the signals A and B could be well detected. These authors suggested that the Mo^{5+}_{6c} and Mo^{5+}_{5c} species exist mainly on the external surface of the HZSM-5 zeolite [27]. In addition, signal A is much more intense than signal B, implying that a large part of the Mo species located on the external surface is in a distorted octahedral coordination.

Running the MDA reaction at 973 K for 0.5 h produced a new, detectable isotropic signal located at $g = 2.003$ (Fig. 1b). As ascribed by Lange et al. [42], this signal was due to the free electrons of condensed aromatic or graphite-like coke and indicated the formation of carbonaceous deposits. With prolonged time on stream from 0.5 h to 1 h, an evident increase in the signal located at $g = 2.003$ (Fig. 1c) was seen, resulting from the formation of more carbon species on the surface of the im-Mo/HZSM-5(H) catalyst. In addition, the overall signal of the Mo^{5+} species became rather complicated. The B signal disappeared completely, indicating further reduction of the square pyramidally coordinated Mo^{5+}_{5c} species on the external surface of the HZSM-5 zeolite. Meanwhile, a new six-line and axially symmetric signal appeared at $g_\perp = 1.983$, $g_\parallel = 1.921$, denoted as signal C, it was attributed mainly to the overall Mo^{5+} signal. Signal C clearly represents superimposed hyperfine structures (HFS), with the splitting of $g_\parallel$ not as severe as the splitting of $g_\perp$. Such splitting lines in the EPR spectra of the MoO_3/HZSM-5 catalysts were reported in only one study [27]. The authors suggested also assigning the splitting signal C to the Mo^{5+} species. The HFS of this signal resulted from the existence of the nearby odd nucleus moment when the Mo^{5+} species are located at positions closely associated with the framework ^{27}Al species ($I = 5/2$). The super-hyperfine interaction between the Mo^{5+} species and the ^{27}Al atoms will lead to splitting of the Mo^{5+} EPR signal. Therefore, the Mo species corresponding to the sextet-splitting signal C are ascribed to the mononuclear Mo^{5+} cation that has a particular interaction with the framework Al species and is located in the channels of HZSM-5. The assignment is very similar to those reported in the cases of Cr/HZSM-5 and Cu/HZSM-5 [43–45]. Recently, two-dimensional ^{27}Al MAS NMR was used to study the Al species on MoO_3/HZSM-5 catalysts prepared by impregnation, and the experimental results indicated a strong interaction between supported Mo species and the framework Al atoms through a Mo–O–Al bonds [46]. Results of the ^1H MAS NMR experiments suggested that the Mo species would migrate into the channels during thermal treatment and replace the Brönsted acid sites, leading to a decreased number of Brönsted acid sites [47]. Therefore, it is reasonable to attribute signal C to the Mo species associated with the Brönsted acid sites, most of which are inside the channels of the HZSM-5 zeolite. But signal C did not appear when the im-MoO_3/HZSM-5 catalyst was treated in hydrogen at 623 K, suggesting that the reduction of the Mo^{6+} species associated with Brönsted acid sites to the Mo^{5+} species is much more difficult than the reduction of the Mo^{6+} species on the external surface of the HZSM-5 zeolite. Moreover, after the catalyst sample was treated with methane for 30 min, signal A, located at $g_\perp = 1.950$ and $g_\parallel = 1.894$ and corresponding to the Mo^{5+}_{6c} species in distorted octahedral coordination, exhibited a significant change in shape. The $g_\perp$ tensor of this signal split and showed the same HFS as in signal C. To simplify the discussion, signal A, with sextet spitting, is denoted as signal D. The g tensors of signal D were almost the same as those of signal A, indicating that the distorted octahe-

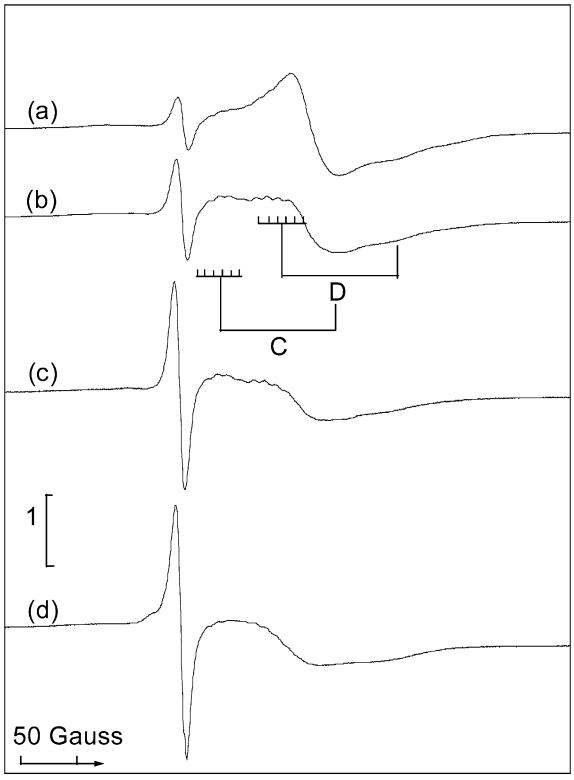

Fig. 2. EPR spectra of the im-Mo/HZSM-5(M) catalyst after running the MDA reaction for 0.5 h (a), 1 h (b), 2 h (c), and 4 h (d) at 973 K.

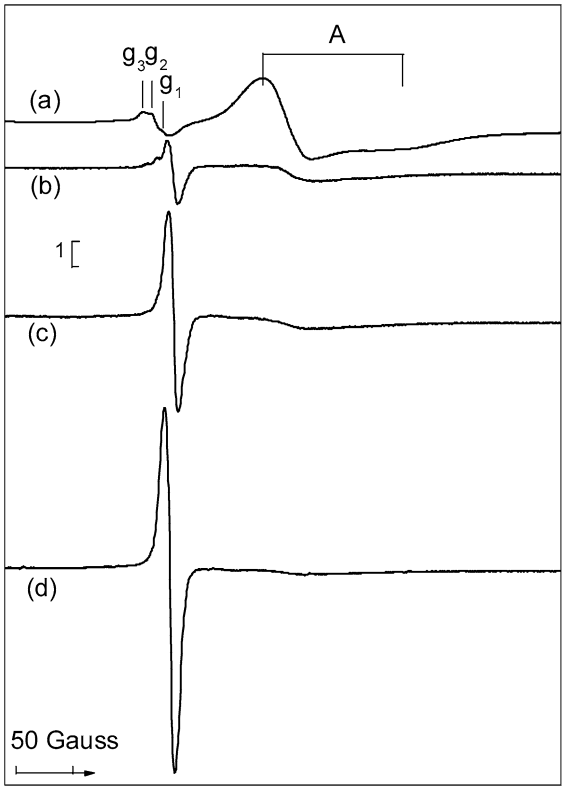

Fig. 3. EPR spectra of the mm-MoO_3/HZSM-5 sample after prereduced with H_2 at 623 K for 6 h (a), and the mm-Mo/HZSM-5(H) catalyst after running the MDA for 0.5 h (b), 1 h (c), and 2 h (d) at 973 K.

drally coordinated Mo^{5+} species located at the external surface of the HZSM-5 zeolite did not change its coordination environment with the oxygen ligands. The splitting represented by signal D suggests that the interaction between the Mo species and the zeolite was strengthened during the methane treatment. The unpaired electrons of the Mo species likely were affected by the Al atoms through the bridged oxygen.

The overall Mo^{5+} signal decreased when the reaction time was increased from 0.5 to 1 h. It should be noted that the decrease in the intensity of signal D was more severe than that in signal C, implying that further reduction of the Mo^{5+} species on the external surface of the HZSM-5 was easier than that of the Mo^{5+} species associated with Brönsted acid sites and located in the zeolite channels. On further increases in reaction time from 1 to 2 h or from 2 to 4 h, the intensities of the splitting signals C and D decreased continuously, particularly for the high field signal D (Figs. 1d and e).

The symmetrical signal located at $g = 2.003$ and ascribed to the carbonaceous deposits as well as the signal of the Mo^{5+} species was clearly visible after the im-Mo/HZSM-5(M) catalyst was treated in CH_4 at 973 K for 30 min (Fig. 2a). The overlapping signal for the Mo^{5+} species was composed mainly of two signals A and B. A weak signal C could be detected, but the superimposed splitting structures of this signal could not be readily distinguished. With prolongation of the reaction time to 1 h, the intensity of signal C increased significantly, and the HFS of this signal became quite clear. Meanwhile, signal A exhibited sextet-splitting structures and formed signal D; however, signal D of the im-Mo/HZSM-5(M) sample was not as intense as that of the im-Mo/HZSM-5(H) sample (Fig. 2b). Further prolonging the treatment time led to decreased intensity of the Mo^{5+} signal, especially for the high field signal D.

3.3. EPR characterization of the Mo species on MoO_3/HZSM-5 samples

When a fresh mm-MoO_3/HZSM-5 catalyst was reduced by H_2 at 623 K, only the smooth axial symmetric EPR signal A located at $g_\perp = 1.950$ and $g_\parallel = 1.894$ was detectable (Fig. 3a). Differing from the situation of the im-MoO_x/HZSM-5 catalyst, signal B could hardly be monitored, demonstrating that the distorted and octahedrally coordinated Mo species, Mo_{6c}, was the dominant Mo species on a MoO_3/HZSM-5 catalyst prepared by mechanical mixing. In addition to the signal corresponding to the Mo^{5+} species, a new signal with peaks at $g_1 = 2.004$, $g_2 = 2.012$, and $g_3 = 2.016$ appeared. When MoO_3/SiO_2 catalyst was thermally reduced [48] or photoreduced [49], similar EPR spectra with the same orthorhombic g tensor as in our work could be observed. This signal was attributed to O_2^- species. Later, Howe and co-workers [39,50,51] investigated the Mo species on reduced molybdenum-based catalysts prepared by different methods and found that the O_2^- signal could also be detected when the Mo/HZSM-5 catalyst was prepared by aqueous ion exchange or when a H mordenite was treated by adsorption of $MoCl_5$ and reduced by hydrogen at 723 K. These authors ascribed the signal, according to the indication of the HFS induced by ^{17}O species, to a normal ionic O_2^- radical ad-

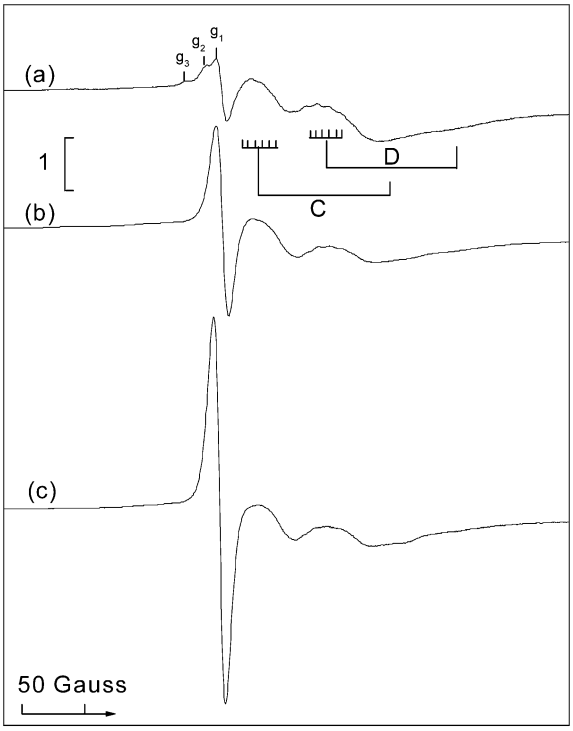

Fig. 4. EPR spectra of the mm-Mo/HZSM-5(M) catalyst after running the MDA reaction for 0.5 h (a), 1 h (b), and 2 h (c) at 973 K.

sorbed asymmetrically on a Mo site. This kind of O_2^- species exists mainly on the external surface of the zeolites, including magnetically equivalent oxygen atoms on Mo-mordenite and inequivalent oxygen atoms on Mo/HZSM-5 [39].

When the MDA reaction was carried out over the mm-Mo/HZSM-5 (H) catalyst at 973 K for 0.5 h, a coke signal appeared at $g = 2.003$, suggesting the decomposition of methane and formation of coke (Fig. 3b). Meanwhile, the intensity of signal A decreased dramatically, indicating a further reduction of the Mo^{5+}_{6c} species. Unfortunately, the Mo signal was too weak to be readily distinguished to determine whether or not it had the splitting HFS. By increasing the reaction time, the EPR signal corresponding to Mo^{5+} species decreased to an extent to which it was hardly detectable. At the same time, the signal of O_2^- species disappeared, and only an extremely prominent coke signal at $g = 2.003$ remained. In addition, the signal C did not appear at all, implying the absence of Mo species associated with the Brönsted acid sites on the mm-Mo/HZSM-5 (H) catalyst.

Fig. 4 shows the EPR spectra recorded after the mm-Mo/HZSM-5(M) catalyst was treated in methane at 973 K. When the reaction was carried out for 30 min, the signal of the O_2^- species with characteristic $g_1 = 2.004$, $g_2 = 2.012$, and $g_3 = 2.021$, the signal of coke at $g = 2.003$ and the Mo^{5+} signals (including C and D) could be observed (Fig. 4a). In the simple ionic description of adsorbed O_2^- species, the g_3 components could all be identified as g_{zz} [52]. The signal in Fig. 4a had a higher g_{zz} value (2.021) than the g_{zz} value of 2.016 in Fig. 3a, implying that the O_2^- species were located on the Mo species with lower coordination. Howe et al. [39] found that the O_2^- species formed in the channels of the Mo-mordenite and Mo/HZSM-5 catalyst had a g tensor with $g_{xx} = 2.004$, $g_{yy} = 2.011$, and $g_{zz} = 2.021$. These results are quite similar to ours. Thus, it seems quite reasonable to ascribe the detected O_2^- signal on mm-Mo/HZSM-5(M) to the O species associated with Mo atoms in a lower coordination environment, rather than to hexacoordinated Mo atoms located on the internal surface of the HZSM-5 zeolite. The appearance of the O_2^- signal with $g_1 = 2.004$, $g_2 = 2.012$, and $g_3 = 2.021$ indicates that on the mm-Mo/HZSM-5(M) catalyst, the Mo oxide species could migrate from the external surface into the channels of the HZSM-5 zeolite. In contrast, two poorly resolved splitting Mo^{5+} signals, C and D, could be detected on the spectrum of the mm-Mo/HZSM-5(M) catalyst, indicating that the Mo species associated with the Brönsted acid sites could form on the mm-MoO_3/HZSM-5 catalyst during reduction in a methane flow. Xu et al. [27] investigated the EPR spectra of the MoO_3/HZSM-5 catalysts with various Mo loadings and found that the HFS were related to the dispersion of the Mo species. The better the Mo species are dispersed, the clearer the splitting structures [27]. The different HFS of signals C and D in Figs. 2 and 4 reflect that the Mo species on the im-Mo/HZSM-5(M) catalyst had a better dispersion than those on the mm-Mo/HZSM-5(M) catalyst. With an increasing in time on stream from 0.5 to 1 h, and then to 2 h, the O_2^- signal vanished but the coke signal increased, and the Mo^{5+} signal decreased gradually (Figs. 4b and c).

3.4. Catalytic evaluation of Mo/HZSM-5 catalysts in MDA

The effects of H_2 prereduction on the catalytic performance of MDA over Mo/HZSM-5 catalysts prepared by different methods were investigated. The depletion rate of methane and the selectivity of BTX (benzene, toluene, and xylene) are shown in Fig. 5. The methane conversion rate over the im-Mo/HZSM-5(M) decreased from 2.4 to 1.2 μmol/(g_{cat} s) after the reaction was run for 24 h. However, on the im-Mo/HZSM-5(H) catalyst, the depletion rate of methane remained at 1.9 μmol/(g_{cat} s) after 24 h on stream (Fig. 5A). In the same way, the selectivity of BTX (predominately benzene) over the im-Mo/HZSM-5(H) was higher and remained at a more stable level than that on the im-Mo/HZSM-5(M) catalyst (Fig. 5B). Obviously, for the MoO_3/HZSM-5 catalyst prepared by impregnation, pretreatment in hydrogen at 623 K for 6 h could greatly improve catalytic activity, stability, and selectivity to monocyclic hydrocarbons.

The methane conversion rate and the BTX selectivity on the mm-Mo/HZSM-5(M) catalyst were comparable with those on the im-Mo/HZSM-5(M) catalyst. Methane also could be activated on the mm-Mo/HZSM-5(H) catalyst pretreated by hydrogen at 623 K, but the conversion rate of methane was only ca. 0.5 μmol/(g_{cat} s), and the methane conversion scarcely changed during an 8-h reaction. More importantly, <8% of the methane molecules activated on the mm-Mo/HZSM-5(H) catalyst could be transformed into BTX, and carbonaceous deposits were the main products. Evidently, after pretreatment with hydrogen at 623 K, the mm-MoO_3/HZSM-5 catalyst had nearly lost its ability to catalyze the reaction of MDA.

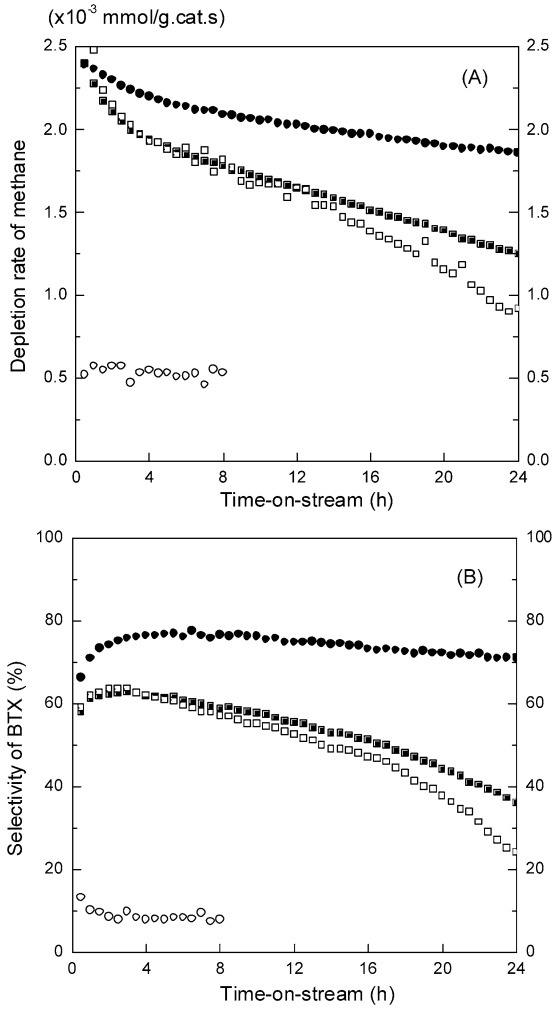

Fig. 5. Methane depletion rate (A) and BTX selectivity (B) over Mo/HZSM-5 catalysts prepared by different methods and pre-activated through different procedures: (■) im-Mo/HZSM-5 (M), (●) im-Mo/HZSM-5 (H), (□) mm-Mo/HZSM-5 (M) catalyst, and (○) mm-Mo/HZSM-5 (H).

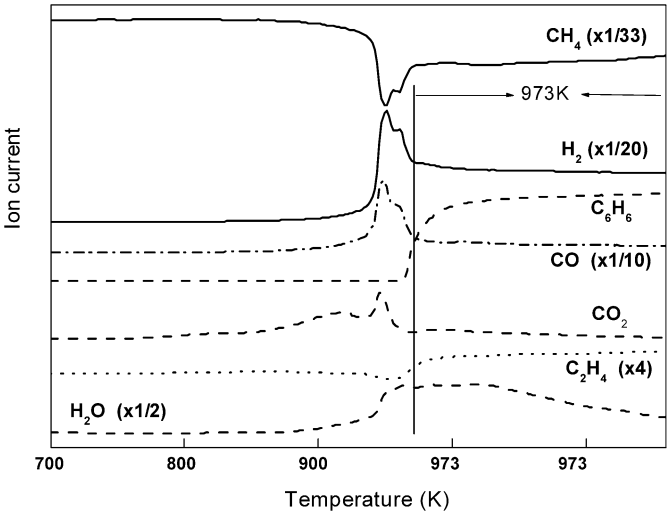

Fig. 6. TPSR profile of the im-Mo/HZSM-5 (M) catalyst.

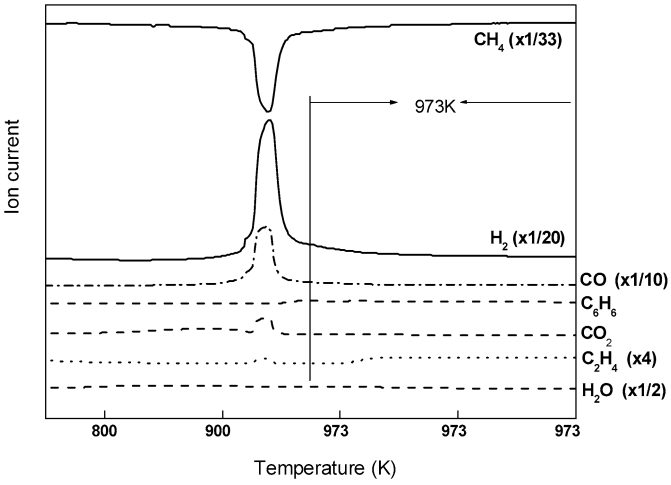

Fig. 7. TPSR profile of the mm-Mo/HZSM-5 (H) catalyst.

3.5. CH_4-TPSR results

The CH_4-TPSR profiles of the im-Mo/HZSM-5 (M) catalyst are presented in Fig. 6. At 870 K, the Mo oxide species began to be reduced by methane, accompanied by the formation of CO_2, CO, H_2O, and H_2. When the temperature was increased to 963 K, formation of ethylene and benzene occurred. As pointed out by Solymosi et al. [5–7] and Lunsford et al. [20,21], the transformation of Mo oxide to active Mo species and the formation of aromatics are dominant in this stage (i.e., the induction period of MDA). The TPSR profiles of the im-Mo/HZSM-5(H) and mm-Mo/HZSM-5(M) catalysts are similar to that of the im-Mo/HZSM-5(M) catalyst (profiles not shown here). However, the CH_4-TPSR profile of the mm-Mo/HZSM-5(H) catalyst (Fig. 7) is quite different from those of the other three catalysts. In the temperature range 870–963 K, methane consumption was clearly observed, together with H_2, CO, and CO_2 formation. Apparently, the Mo oxide species supported on HZSM-5 zeolite was reduced by methane in this stage. With further temperature increases, methane conversion and hydrogen formation reached relatively stable values, and the ethylene became detectable. Unfortunately, the expected product, benzene, was barely detected, even though the mm-Mo/HZSM-5(H) catalyst was treated in methane at 973 K for 1 h.

4. Discussion

4.1. Coke formation during the MDA reaction

As illustrated in Fig. 8, the coked im-Mo/HZSM-5(M), im-Mo/HZSM-5(H), and mm-Mo/HZSM-5(M) catalysts exhibited three TPO peaks, at 732, 784, and 831 K, respectively. According to the TPO profiles of our serial studies on carbonaceous deposits on Mo/HZSM-5, Mo/TiO_2, and Mo/MCM-22 after the MDA reactions were run, the carbon species burning at high temperatures (above 800 K) were mainly those formed on the Brönsted acid sites of the zeolites, whereas the carbonaceous deposits burning at lower temperatures were usually located on the Mo carbide or Mo oxycarbide [28,29,53,54]. The coke oxidized in the early stage at 732 K was deposited on the Mo

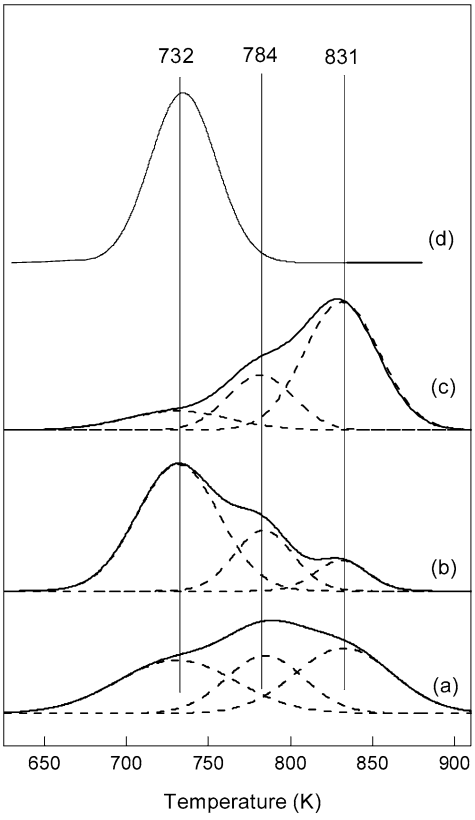

Fig. 8. TPO profiles and deconvolution peaks of the coked Mo/HZSM-5 catalysts after running the reaction at 973 K for 1 h: (a) im-Mo/HZSM-5 (M), (b) im-Mo/HZSM-5 (H), (c) mm-Mo/HZSM-5 (M), and (d) mm-Mo/HZSM-5 (H).

carbide species locating at the external surface of the HZSM-5 zeolite, whereas the TPO peak at 784 K possibly corresponded to the coke associated with the Mo species in the HZSM-5 channels. In the initial period of MDA, the Mo oxide species were reduced and carburized by methane and formed active Mo species, Mo carbide, or Mo oxycarbide, as generally accepted [17–21]. The activated methane molecules could readsorb and anchor on the active Mo species to form coke. At the end of the induction period, benzene was observed, as illustrated in the CH_4-TPSR profiles of the im-Mo/HZSM-5 catalysts shown in Fig. 6. At the same time, further dehydrogenation and oligomerization of monocyclic aromatic products also could lead to the deposition of aromatic-type carbon species on the Brönsted acid sites. Thus, the TPO peak at the high temperature (831 K) appeared. It has been shown that the carbon deposits associated with the Mo species were reactive and reversible, but the coke formed on the Brönsted acid sites was inert and irreversible. The latter is a crucial factor for the deactivation of the Mo/HZSM-5 catalysts [55]. When the im-MoO_3/HZSM-5 catalyst was pretreated with hydrogen at 623 K, more carbon was deposited on the external surface of the Mo species and less coke was formed on the Brönsted acid sites (see Fig. 8), suggesting that H_2 pretreatment could improve the formation of reactive carbon and suppress the deposition of inert coke.

On a fresh mm-MoO_3/HZSM-5 catalyst, all Mo species usually exist on the external surface of the HZSM-5 zeolite. However, the coked mm-Mo/HZSM-5(M) exhibited three TPO peaks, similar to the im-Mo/HZSM-5 catalysts. The deposited coke was located on the Mo species inside the HZSM-5 channels, indicating migration of the Mo species into the zeolite channels during the treatment with methane. The coked mm-Mo/HZSM-5(H) catalyst presented a single TPO signal at 732 K, as shown in Fig. 8d, differing from the triple-peak signal shown by the other catalysts. Unquestionably, the single peak should be assigned to the carbonaceous deposits associated with the Mo species locating at the external surface of the HZSM-5 zeolite. No signals appeared corresponding to the coke on the internal surface of the Mo species, suggesting that the reduction in hydrogen at 623 K prevented the external-surface Mo species from diffusing into the channels. As shown in Figs. 5 and 8, on the mm-Mo/HZSM-5(M) catalyst, methane molecules were activated and transformed into benzene, whereas on the mm-Mo/HZSM-5(H) catalyst, methane molecules were also activated but were transformed mainly into coke. It is generally accepted that the activation of methane and formation of initial C_2 hydrocarbons occur on the reduced MoO_x species, whereas the production of mono-cyclic aromatics is catalyzed by the Brönsted acid sites of the HZSM-5 zeolite [4–15]. Inferring from our results, the Mo species locating in the HZSM-5 channels are contiguous with the Brönsted acid sites, which play very important roles in the formation of aromatics.

4.2. The active Mo species for MDA

EPR results have revealed three kinds of Mo species on the MoO_3/HZSM-5 catalyst prepared by impregnation: the Mo^{6+}_{6c} species in distorted octahedral coordination, the Mo^{6+}_{5c} species in square pyramidal coordination, and the Mo^{6+} species associated with the Brönsted acid sites. The former two Mo species exist mainly on the external surface of the HZSM-5 zeolite and can be easily reduced to Mo^{5+}, whereas the latter resides primarily inside the channels. Furthermore, during the MDA reaction at 973 K, two kinds of Mo^{5+} species are present on the Mo/HZSM-5 catalyst, one derived from the Mo_{6c} species interacting with the HZSM-5 zeolite and the other associated with the Brönsted acid sites. With progression of the reaction, a part of the Mo^{5+} species, mainly the Mo species on the external surface of the HZSM-5 zeolite, is further reduced by methane. The quantitative EPR results, obtained by double-integrating the overall Mo^{5+} signal, are shown in Fig. 9. Evidently, the amount of the overall Mo^{5+} species is much greater on im-Mo/HZSM-5(H) than on im-Mo/HZSM-5(M). ^{1}H MAS NMR results have revealed that the amounts of all hydroxy groups on im-MoO_3/HZSM-5 remain unchanged after H_2 prereduction at 623 K (spectra not shown here): therefore, further migration and dispersion of the Mo species on the external surface or into the channels of the HZSM-5 zeolite did not occur during H_2 prereduction. As is well known, stable β-Mo_2C species in hexagonally close-packed (hcp) structures can be attained by temperature-programmed treatment of MoO_3 species from room temperature to 983 K in a methane flow, whereas metastable α-MoC_{1-x} species in face-centered cubic

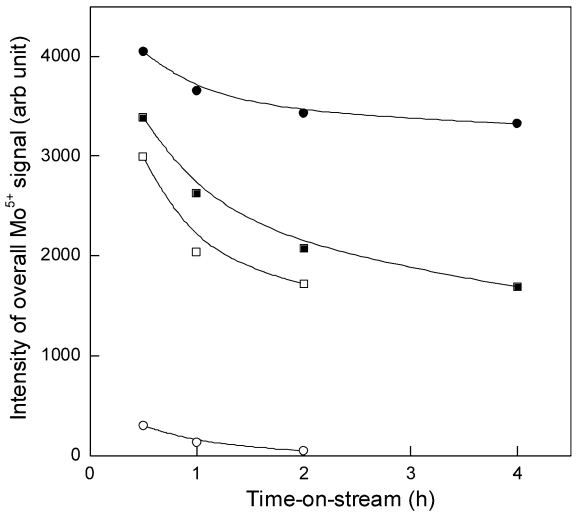

Fig. 9. The intensity of EPR signals of all Mo^{5+} species on the Mo/HZSM-5 catalysts after the reaction at 973 K with time on stream: (■) im-Mo/HZSM-5 (M), (●) im-Mo/HZSM-5 (H), (□) mm-Mo/HZSM-5 (M), and (○) mm-Mo/HZSM-5 (H).

(fcc) structure can be formed from MoO_3 species through reduction in hydrogen flow at 623 K and subsequent carburization in methane [56–58]. Our previous work has demonstrated that the Mo species associated with the Brönsted acid sites can be only partially reduced by CH_4 to form the MoC_xO_y species and is still associated with the Brönsted acid sites [27]. Therefore, the Mo^{5+} species recorded from the im-Mo/HZSM-5 catalysts during the reaction are associated with the HZSM-5 and in the form of MoC_xO_y. The MoC_xO_y species is probably in an hcp structure on im-Mo/HZSM-5(M) because of its reduction with methane and in an fcc structure on the im-Mo/HZSM-5(H) because of its pretreatment in hydrogen. Reduction of the Mo species in an fcc structure is much more difficult than reduction of those in an hcp structure, causing a far greater amount of Mo^{5+} species to remain on the im-Mo/HZSM-5(H) catalyst than on the im-Mo/HZSM-5(M) catalyst. Meanwhile, higher activity, better selectivity to aromatics, and better stability were attained over the im-Mo/HZSM-5(H) catalyst, as shown in Fig. 5. The differences in catalytic performance may stem from the fact that the MoO_xC_y species with an fcc structure exhibit higher activity and better stability than those with an hcp structure for the reaction of MDA.

On fresh MoO_3/HZSM-5 catalyst prepared by mechanical mixing, the Mo species exist mainly in octahedral coordination, just as they do in bulk MoO_3. Under a reducing atmosphere due to the presence of methane and high temperature, the MoO_3 could disperse well on the surface of zeolite and migrate into the channels to interact with the Brönsted acid sites, resulting in the formation of Mo species associated with the Brönsted acid sites, as well as a change in the coordination environment of the Mo species. This would lead to the appearance of EPR signal C in Fig. 4. At the same time, the interaction between the Mo species remaining on the external surface of the HZSM-5 and the zeolite is strengthened, producing signal D. Based on the foregoing discussion, the MoO_xC_y species on mm-Mo/HZSM-5(M) is probably in an hcp structure, and it is not surprising that mm-Mo/HZSM-5(M) and im-Mo/HZSM-5(M) exhibit similar catalytic performance. When mm-MoO_3/HZSM-5 was reduced by H_2 at 623 K and then treated by methane at 973 K, only a little Mo^{5+} species appeared on mm-Mo/HZSM-5(H) (Fig. 9). The TPR and TPO results (Table 1 and Fig. 8) reveal that pretreatment in hydrogen could suppress the migration of the Mo species into the HZSM-5 channels. The crystalline MoO_3 existing on the external surface of the zeolite was possibly transformed to an fcc α-MoC_{1-x} carbide via reduction in hydrogen at 623 K and then carbonization in methane. On the other hand, mm-Mo/HZSM-5(H) exhibited very poor performances in MDA (Fig. 5). During the entire 8-h reaction, the methane depletion rate on mm-Mo/HZSM-5(H) did not change, indicating that the fcc α-MoC_{1-x} species could activate methane regardless of the significant coke deposition. Unfortunately, the amount of monocyclic aromatics formed on the mm-Mo/HZSM-5(H) catalyst was rather small because of the long distance between the Mo carbide species and the Brönsted acid sites. Consequently, both the active Mo species and the vicinal Brönsted acid sites are indispensable for the reaction of methane dehydroaromatization.

5. Conclusions

Thee kinds of Mo species exist on the MoO_3/HZSM-5 catalyst prepared by impregnation: the distorted octahedrally coordinated Mo_{6c} species, the square pyramidally coordinated Mo_{5c} species, and the Mo species associated with Brönsted acid sites. The former two Mo species exist mainly on the external surface of the HZSM-5 zeolite, whereas the latter resides primarily in the channels. The Mo species associated with the HZSM-5 zeolite can be only partially reduced by methane to form the MoC_xO_y species, which play crucial roles in the reaction of methane dehydroaromatization. The Mo species with an fcc structure are not as easily reduced by methane and are more efficient in MDA than the Mo species with an hcp structure. Prereduction of im-MoO_3/HZSM-5 with H_2 at 623 K can lead to a topotactic transformation of the Mo species from the hcp structure to the fcc structure, thereby creating a Mo/HZSM-5 catalyst with higher activity for methane conversion, better selectivity to aromatics, and better stability.

On a MoO_3/HZSM-5 catalyst prepared by mechanical mixing, the Mo species located on the external surface of the zeolite can diffuse and migrate into the channels to form Mo species associated with the Brönsted acid sites under a methane atmosphere at high temperature. However, the reduction in hydrogen at 623 K will suppress the migration of the Mo species, resulting in the catalytic inactivity of Mo/HZSM-5 in the MDA reaction due to the long distance between the Mo active species and the Brönsted acid sites.

Acknowledgments

Financial support from the Ministry of Science and Technology of China (contracts G1999022406 and 2005CB221400), the Natural Science Foundation of China (grant 20473086), and the BP-CAS (China) Joint Center is gratefully acknowledged.

References

[1] L. Wang, L. Tao, M. Xie, G. Xu, J. Huang, Y. Xu, Catal. Lett. 21 (1993) 35.
[2] Y. Xu, L. Lin, Appl. Catal. A 188 (1999) 53.
[3] Y. Xu, X. Bao, L. Lin, J. Catal. 216 (2003) 386.
[4] Y. Xu, S. Liu, L. Wang, M. Xie, X. Guo, Catal. Lett. 30 (1995) 135.
[5] F. Solymosi, A. Erdohelyi, A. Szöke, Catal. Lett. 32 (1995) 43.
[6] A. Szöke, F. Solymosi, Appl. Catal. A 142 (1996) 361.
[7] F. Solymosi, A. Szöke, Catal. Lett. 39 (1996) 157.
[8] F. Solymosi, J. Cserényi, A. Szöke, T. Bánsági, A. Oszkó, J. Catal. 165 (1997) 150.
[9] D. Wang, J.H. Lunsford, M.P. Rosynek, J. Catal. 169 (1997) 347.
[10] Y. Shu, D. Ma, L. Xu, Y. Xu, X. Bao, Catal. Lett. 70 (2000) 67.
[11] Y. Shu, D. Ma, X. Liu, X. Han, Y. Xu, X. Bao, J. Phys. Chem. B 104 (2000) 8245.
[12] S. Liu, Q. Dong, R. Ohnishi, M. Ichikawa, Chem. Commun. (1997) 1455.
[13] L. Wang, R. Ohnishi, M. Ichikawa, J. Catal. 190 (2000) 276.
[14] J. Zeng, Z. Xiong, H. Zhang, G. Lin, K. Tsai, Catal. Lett. 53 (1998) 119.
[15] B.M. Weckhuysen, D. Wang, M.P. Rosynek, J.H. Lunsford, J. Catal. 175 (1998) 338.
[16] B.M. Weckhuysen, D. Wang, M.P. Rosynek, J.H. Lunsford, J. Catal. 175 (1998) 347.
[17] C. Zhang, S. Li, Y. Yuan, W. Zhang, T. Wu, L. Lin, Catal. Lett. 56 (1998) 207.
[18] Y. Shu, Y. Xu, S. Wong, L. Wang, X. Guo, J. Catal. 170 (1997) 11.
[19] L. Chen, L. Lin, Z. Xu, X. Lian, T. Zhang, X. Li, J. Catal. 157 (1995) 190.
[20] D. Wang, J.H. Lunsford, M.P. Rosynek, Top. Catal. 3 (1996) 289.
[21] B.M. Weckhuysen, M.P. Rosynek, J.H. Lunsford, Catal. Lett. 52 (1998) 31.
[22] R.W. Borry III, Y.H. Kim, A. Huffsmith, J.A. Reimer, E. Iglesia, J. Phys. Chem. B 103 (1999) 5787.
[23] Y.H. Kim, R.W. Borry III, E. Iglesia, Microporous Mesoporous Mater. 35–36 (2000) 495.
[24] W. Li, G. Meitzner, R.W. Borry III, E. Iglesia, J. Catal. 191 (2000) 373.
[25] W. Ding, S. Li, G. Meitzner, E. Iglesia, J. Phys. Chem. B 105 (2001) 506.
[26] W. Ding, G. Meitzner, E. Iglesia, J. Catal. 206 (2002) 14.
[27] D. Ma, Y. Shu, X. Bao, Y. Xu, J. Catal. 189 (2000) 314.
[28] H. Liu, T. Li, B. Tian, Y. Xu, Appl. Catal. A 213 (2001) 103.
[29] H. Liu, L. Su, H. Wang, W. Shen, X. Bao, Y. Xu, Appl. Catal. A 236 (2002) 263.
[30] G.C. Bond, S.F. Tahir, Appl. Catal. A 105 (1993) 281.
[31] J.R. Regalbuto, J.W. Ha, Catal. Lett. 29 (1994) 189.
[32] C.C. Williams, J.G. Ekerdt, J.M. Jehng, J. Phys. Chem. 95 (1991) 8791.
[33] F. Barath, M. Turki, V. Keller, G. Maire, J. Catal. 185 (1999) 1.
[34] J.S. Lee, S.T. Wyama, M. Boudart, J. Catal. 106 (1987) 125.
[35] F. Barath, M. Turki, V. Keller, G. Maire, J. Catal. 185 (1999) 1.
[36] S. Tang, H. Chen, J. Lin, K.L. Tan, Catal. Commun. 2 (2001) 31.
[37] R.F. Howe, I.R. Leith, J. Chem. Soc., Faraday Trans. 69 (1973) 1967.
[38] C. Louis, M. Che, J. Phys. Chem. 91 (1987) 2875.
[39] M.M. Huang, J.R. Johns, R.F. Howe, J. Phys. Chem. 92 (1988) 1291.
[40] M. Che, J.L. McAteer, A.J. Tench, J. Chem. Soc., Faraday Trans. 74 (1978) 2378.
[41] M. Che, M. Fournier, J.P. Launay, J. Phys. Chem. 71 (1979) 1954.
[42] J.P. Lange, A. Gutsze, H.G. Karge, J. Catal. 114 (1988) 136.
[43] A.V. Kucherov, A.A. Slinkin, Zeolites 7 (1987) 38.
[44] B. Wichterlova, J. Dedecek, A. Vondrova, J. Phys. Chem. 99 (1995) 1065.
[45] J. Dedecek, Z. Sobalik, Z. Tvaruzkova, D. Kaucky, B. Wichterlova, J. Phys. Chem. 99 (1995) 16327.
[46] D. Ma, X. Han, D. Zhou, Z. Yan, R. Fu, Y. Xu, X. Bao, H. Hu, S.C.F. Au-Yeung, Chemisty 8 (2002) 4557.
[47] W. Zhang, D. Ma, X. Han, X. Liu, X. Bao, X. Guo, X. Wang, J. Catal. 188 (1999) 393.
[48] M. Che, A.J. Tench, C. Naccache, J. Chem. Soc., Faraday Trans. 70 (1974) 263.
[49] Y. Ben Taarit, J.H. Lunsford, J. Phys. Chem. 77 (1973) 780.
[50] S.R. Seyedmonir, R.F. Howe, J. Chem. Soc., Faraday Trans. 80 (1984) 2269.
[51] S.R. Seyedmonir, R.F. Howe, J. Chem. Soc., Faraday Trans. 80 (1984) 87.
[52] M. Che, A.J. Tench, Adv. Catal. 32 (1985) 1.
[53] D. Ma, Y. Shu, M. Cheng, Y. Xu, X. Bao, J. Catal. 194 (2000) 105.
[54] D. Ma, D. Wang, L. Su, Y. Shu, Y. Xu, X. Bao, J. Catal. 208 (2002) 260.
[55] R. Ohnishi, S. Liu, Q. Dong, L. Wang, M. Ichikawa, J. Catal. 182 (1999) 92.
[56] C. Bouchy, S.B. Derouane-Abd Hamid, E.G. Derouane, Chem. Commun. 2 (2000) 125.
[57] S.B. Derouane-Abd Hamid, J.R. Anderson, I. Schmidt, C. Bouchy, C.J.H. Jacobsen, E.G. Derouane, Catal. Today 63 (2000) 461.
[58] C. Bouchy, I. Schmidt, J.R. Anderson, C.J.H. Jacobsen, E.G. Derouane, S.B. Derouane-Abd Hamid, J. Mol. Catal. A 163 (2000) 283.